Morphological communication for swarms

Asheesh Sharma[1], Sabine Hauert[1,2] and Helmut Hauser[1,2]

[1]Dept. of Engineering Mathematics, University of Bristol, Bristol, U.K.
[2]Dept. of Engineering Mathematics, Bristol Robotics Laboratory, Bristol, U.K.
as16542@my.bristol.ac.uk
sabine.hauert@bristol.ac.uk
helmut.hauser@bristol.ac.uk

Abstract

Robotic swarms rely on local communication between agents to exhibit cooperative emergent behaviours. Local communication is typically implemented with technologies that require dedicated electronics, that can be expensive and difficult to miniaturise or mass-produce. Computational resources are then needed to transform this information into a robot action following a set of rules, further limiting swarm lifetime (battery) and scalability. In this paper, we propose an alternative approach by using the concept of morphological computation (computation through morphology) for local communication in swarms. In such a swarm, local communication is implemented as simple mass-spring-damper systems between agents, instead of electronics. We test this approach in a simple scenario where a swarm has to squeeze through a narrow gap while floating on water. We tested different types of swarms (with different levels of control) and measured their average performance and energy efficiency. We found that by offloading the majority of communication and information processing to the morphology, swarms can exhibit interesting, emergent, cooperative behaviour to solve the given task.

Introduction

Swarm engineering enables a collection of simple agents that react only to local information to perform complex behaviours (Kaynaklarından et al., 2005). Applications of robot swarms include search and rescue (Hauert et al., 2014; Couceiro, 2017; Li et al., 2009a), exploration (Hinchey et al., 2007), environmental monitoring (Duarte et al., 2016), and construction (Slavkov et al., 2018). We refer to Brambilla et al. (2013) for an in-depth review.

A key component of swarms is local communication between neighboring agents. In robotic swarms, this communication is typically implemented using wireless technologies, for example WiFi (Hauert et al., 2010), Zigbee (Cianci et al., 2006), or other radio based technologies (Li et al., 2009b; Tutuko and Nurmaini, 2014). While other systems have been proposed using light (Rubenstein et al., 2014; Roberts et al., 2009; Trenkwalder et al., 2020), or sensory readings such as vision (Floreano et al., 2007; Garattoni and Birattari, 2018).

However, a drawback of such implementations is that they often require dedicated electronics that can be expensive and difficult to miniaturise or mass-produce; leading to scalability issues of such swarms to large numbers (Hauert and Bhatia, 2014).

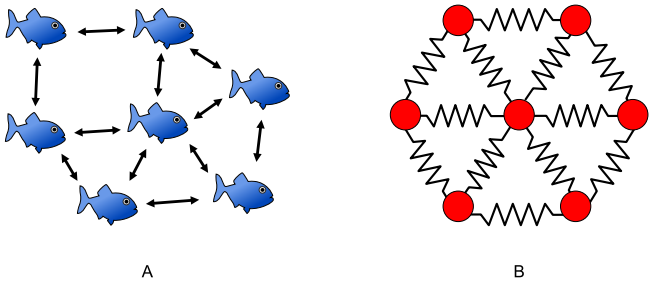

Figure 1: Local communication A: Robotic fish transmitting their position to neighboring robots to maintain a formation. B: The same principle can be represented as robots constrained by compliant connecting element like mass-spring damper systems. The preferred distances are encoded in the resting lengths.

Modular self-reconfigurable robotics (MSRR) is another approach where multiple simpler agents work together to achieve a goal. Communication in this case is established by physical links. For example, Brown et al. (2002) developed a self-docking group of robots called millibots which use 2D latching mechanisms. However, the distance between agents is physically fixed and doesn't allow for a smooth, dynamic change of size. We refer to Seo et al. (2019); Alattas (2018); Chennareddy et al. (2017) for a survey on modular robotics.

In this paper, we propose to use morphological communication. Instead of swarms composed of freely moving agents, e.g. as in schools of fish (see Fig.1A), we propose swarms of physically connected robots through compliant links that communicate through these connections via mechanical forces (see Fig.1B). We implemented simulations of such swarms by connecting mass-points with spring-damper systems. These connections impose a constraint that forces the individuals to maintain a certain distance from each other. More specifically, the spring-damper systems react naturally to compression and elongation by

exerting a counteracting force on the connected individuals. Therefore, by controlling the physical properties of the spring-damper system (i.e. stiffness, damping, and a particular resting length) a desired distance can be dynamically maintained without any additional actuation force. Technically, assuming that both stiffness and damping are linear, the connections represent mechanical implementations of a PD controller.

Besides maintaining a certain distance, the spring-damper systems also function as mechanical relays of information. For example, transmitting information about a local collision at the border of the swarm through the networks in the form of vibrations. As a result, the proposed systems does not need dedicated electronic parts for communication or localization. The idea of communicating through mechanical structures is often referred to as *morphological communication* (Rieffel et al., 2010).

Mechanisms which exploit morphological communication have been studied previously. For example, Umedachi et al. used a design principle called protoplasmic conservation to build a series of robots inspired by slime-molds (Umedachi et al., 2010a,b; Ishiguro et al., 2008; Umedachi et al., 2013, 2012a,b). The protoplasmic conservation principle enforces global oscillations through the robot's morphology. This played a key role in accomplishing navigational tasks without central control. The robots were made of smaller, alike units connected through compliant mechanisms and arranged in a circle. Both, Rieffel et al. (2010) and Caluwaerts and Schrauwen (2011), have explored the importance of morphological communication in locomotion using tensegrity-like structures. The later built a simulation to demonstrate that morphologies can learn stable locomotion gaits with only linear feedback. Owaki et al. (2013) also explored morphological communication in locomotion. Their work showed that incorporating morphology can be beneficial for coordinated limb movement.

In their paper, Deblais et al. (2018) studied the influence of a particle's chirality on the motion and global behaviour of all the particles when constrained by stationary-rigid and free-to-move compliant boundaries. However, their approach confined the swarms with boundaries which made them a single physical entity interacting with the outside environment indirectly (like sub-cellular systems in a cell). Instead, here we focus on direct physical interactions of robots with the environment by controlling the physical properties of the agent's morphologies.

A different approach of coordinated locomotion in swarms was introduced by Li et al. (2019). They magnetically coupled robots which could only undergo a volumetric oscillation. Using statistical mechanics, they demonstrated that despite the stochastic motion, the swarm exhibited deterministic locomotion. Also in this case, morphological communication played a crucial role in the emergence of this behaviour.

As an alternative to the traditional explanation of morphogenesis in blood vessel growth, Bentley et al. (2014) demonstrated the importance of morphological communication in the strategy employed by the epithelial cells for repairing tissues.

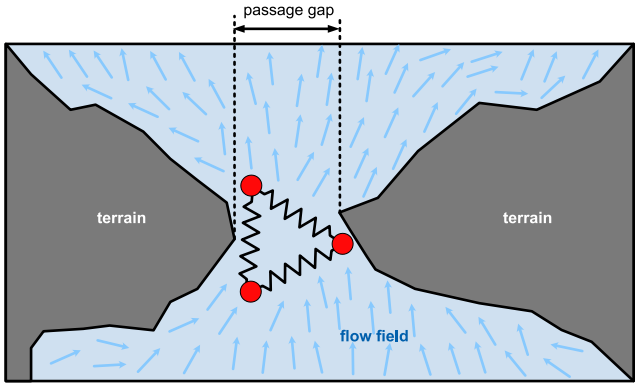

Figure 2: Navigation task the swarm has to solve. The swarm floats on water and has to navigate through a narrow gap. The underlying flow (i.e. vector field of forces) and the terrain are randomly produced and unknown to the swarm.

In this study, we investigate how morphological communication can be exploited in swarms of physically connected robots. Specifically, we define a set of floating agents that are connected through compliant links. Their task is to coordinate their locomotion through a narrow passage leveraging the flow of water (see Fig.2) without a central controller. We investigate and compare a number of different swarm configurations. These configurations range from completely passive swarms to swarms with individuals that are capable of actively shortening their connection length to their neighbours depending on the local touch sensor information (i.e., to retract from an object). We measured (i) the average passing time over a number of random variations of the environment and, (ii) the amount of energy consumed during this process.

Methodology

The aim of this work was to investigate the contribution of morphological communication for the navigation task from Fig.2 and to understand the benefits of compliant connections between agents for coordinated locomotion. We considered a range of different swarm designs with different levels of compliance and autonomy. The 6 chosen designs are summarized in Fig. 3. First, we considered 2 different types of connections, i.e., completely rigid (left in the figure) or compliant connections (right in the figure). The compliant connections were implemented as mass-spring-damper systems. Second, we explored the contribution of local sensing capabilities as opposed to swarms without sensors ("blind" locomotion). The sensors are implemented as simple binary

touch switches using which the individual robots can detect if they are in contact with the surrounding terrain. The sensors are shown as blue half-circles on the outside of robots in Fig. 3. This local touch information triggers the shortening of the respective connections of the sensing agents to its neighbours; resulting in a recoiling behavior from the environment (with rigid connections Fig. 3C and with compliant connections Fig. 3D). In addition, we explored active versions of the swarms that continuously changed all connections lengths in an oscillatory fashion (see Fig. 3E, green wave symbols). The oscillation (indicated by green wave symbols) happened at a fixed amplitude and frequency. Finally, we explored swarms that combined local sensing (i.e. recoiling behaviour) and continuous oscillation (see Fig. 3F, combining blue half-circles and green wave symbols).

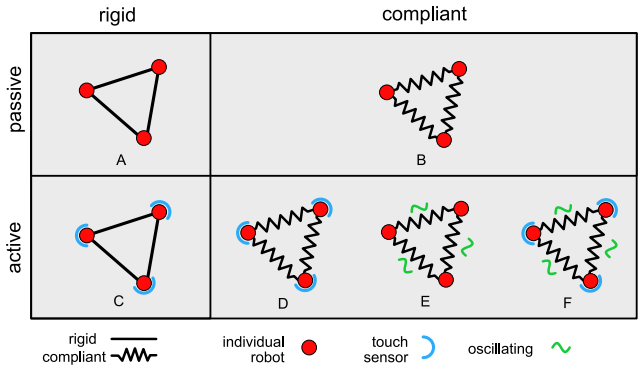

Figure 3: Different types of swarms that have been considered. A: Passive with rigid connections. B: Passive, with compliant connections. C: Rigid connections, which are actively shortened when an obstacle is detected. D: Compliant connections, which are actively shortened when an obstacle is detected. E: Compliant connections continuously oscillating. F: Compliant connections, combining oscillations and the capability to retract.

The summary of types of swarms are shown in Fig. 3. Since we wanted to investigate how morphological communication through compliant connections can lead to coordinated locomotion in swarms, we designed the gap size of the passage (compare Fig. 2) such that only a coordinated effort of individual agents led to a successful passing. Consequently, we empirically determined a gap size that made it just impossible for a completely rigid swarm (Fig. 3A) to pass through. Interestingly, the type of swarms depicted in Fig. 3C, which was also rigid, but had the capability to retract from the walls, was also unlikely to pass such a gap. Specifically, in our experiments only 2 out of 150 simulations of this type of swarm were able cross the finish line. This meant, that for carrying out the task successfully, the swarm would either need compliant connections or some combination of compliant connections and control (retraction and/or oscillation) to pass through the narrow passage.

We defined labels for the different types of swarms to facilitate references later in this paper. They are summarized in Table 1. The labels consist of P (passive) or A (active) as shown by the first and second row in Fig. 3 respectively. The subscripts rec and osc indicate a swarm's capability to avoid obstacles by recoiling and/or oscillating respectively.

Type	Fig.	Passive/Active	Recoil	Oscillation
P	3B	Passive	✗	✗
A_{rec}	3D	Active	✓	✗
A_{osc}	3F	Active	✗	✓
$A_{rec,osc}$	3E	Active	✓	✓

Table 1: Naming convention used for the different types of swarms. Note that rigid swarms Fig. 3A and C were unsuccessful and, hence, don't show up in this table.

Simulation

The simulated task replicated a scenario where the swarm is floating on water and should navigate through a randomly produced passage (see Fig. 2). For every iteration of the experiment, the starting positions, as well the terrain of the environment was randomly produced in order to robustly measure performance of different types of swarms. Correspondingly, a number of repetitions of the experiments were carried out to obtain an average behavior. Please note that the swarms did not have any information about the randomly produced environment and no central controller or explicit central information sharing mechanisms were available.

Environment For the sake of simplicity, the environment was implemented in 2D with a flow-field to represent the dynamics of a water surface (see Fig. 2). As mentioned before, the terrain and the flow, were both randomly produced for every individual trial. The flow-field of the water acts on ev-

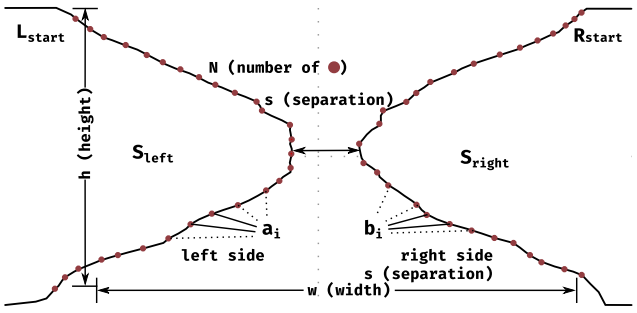

Figure 4: Variables and constants used to randomly generate the terrain for each simulation episode.

ery individual robot of the swarm, but not on the connection as they are assumed to be above the water surface. On average the vector field points upwards toward the goal. As pre-

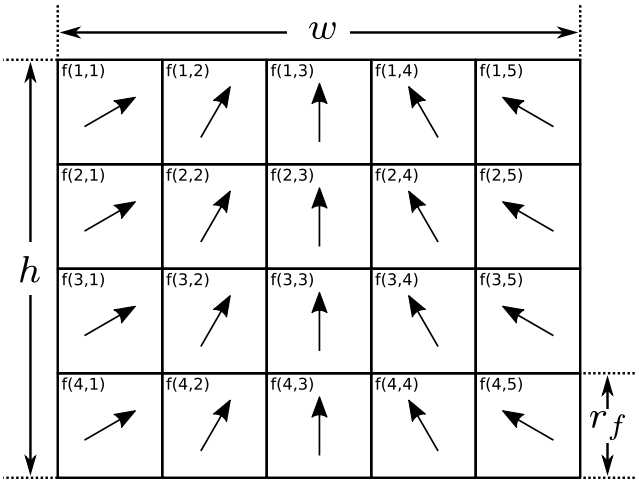

Figure 5: Representation of the flow-field $f(n, m)$ in simulation: The width w and height h are constant for all produced terrains. All grid cells have the same size.

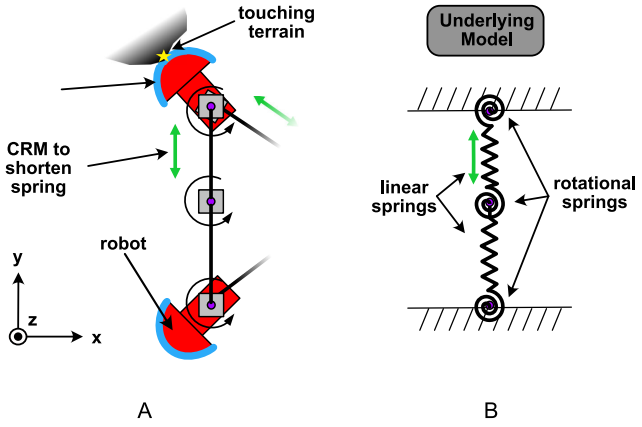

Figure 6: The robot and its components (z-axis points upwards). A: Shows details of the simulated robotic system. When the upper robot touches the terrain, the compliant recoiling mechanism (CRM) is activated (green arrows). Note that only the proximal linear springs are shortened for a fixed amount of time. B: Diagram shows the underlying model using a combination of linear and angular springs to simulate the CRM.

viously pointed out, the gap was designed such that a completely rigid swarm (see Fig. 3A) couln't pass through, i.e., the gap was smaller than the minimal width of the swarm.

The terrain consisted of two surfaces (S_{left} and S_{right}) separated by a distance $s = 20\ cm$ (i.e., the gap), see Fig. 4). In addition, the height h and the width w were fixed to 50 cm, 120 cm respectively. To create the terrain on each side, a sinusoidal wave (half a period) was generated. Then, for every point, the sinusoidal wave was iterated over and the points were displaced with Perlin noise (r) where the next seed (initially 0 for the first point) was incremented with a constant value of 0.2 (see (Perlin, 2002)). To produce different surfaces in each episode (i.e. every time the simulation is restarted because the swarm successfully crossed the terrain or didn't in a given amount of time), the random function internally used by the Perlin noise generator was reseeded. For more details refer to Asheesh and Helmut (2020).

The flow is implemented as a vector field. It is assumed that the flow-field does not change during one episode and that the swarm does not have an impact on the flow-field. The overall surface spanning over the width w and the height h was divided into a regular grid $f(n, m)$ with n rows and m columns (see Fig. 5). Each grid cell had a flow-field vector with a magnitude of unity. In the simulation, there were 768 such flow-field vectors with $n = 24$, $m = 32$, and the height of each grid cell was 25 cm. The entire process including the algorithm is discussed in Asheesh and Helmut (2020). We used Box2D, a 2D physics engine, to implement the simulation (see Catto (2011)).

Swarms The swarms are simulated as individual robots with mechanical connections between them. Fig. 6A shows the relationship in more details. The robots have a semi-circular body which acts as the touch sensor for obstacle detection. Note that this proximity information is binary (touch/no touch) and it is only available to the robots locally, i.e., it is not directly shared with other robots of the swarm. When an obstacle is detected, the robot's compliant recoiling mechanism (CRM) is triggered. This means the connections from this robot to its neighbors will be shortened. Practically, the connection is implemented as two linear springs which are connected with angular springs, see Fig. 6B. Since the touch information is only locally available, the recoiling happens only with the linear spring on the side of the robot that has detected the obstacle. In such a case the CRM will be compressed to a minimum length of 1 centimetre for 50 milliseconds, before it expands back to its nominal length.

In the case of swarms using oscillations, such as A_{osc} and $A_{rec,osc}$, the CRMs are contracted and released continuously. The rate of contraction and relaxation is governed by a standard sinusoidal function $\alpha \sin(\beta)$ with empirically determined values of $\alpha = 5.0$ and $\beta \in [0, \pi]$ being incremented by 0.05 every time-step. When $\beta \to \pi$, it is reset to $\beta = 0$ to complete one oscillation.

In relation to recoiling (obstacle avoidance), the oscillations are switched off as soon as a robot touches the surface and resumed after the same delay of 50 milliseconds for which the CRM remains contracted. In Fig 3E (A_{osc}) the compliant connections are continuously oscillating between completely contracted to relaxed independent of any sensory information. While in swarms of the type $A_{rec,osc}$ as depicted in Fig 3F, both the oscillation and the recoiling behaviors are combined. Any action of the CRM will intro-

duce forces that will be communicated to the other robots through the mechanical, soft connections. Although the collision detection happens locally, through the compliant connections, the agents will be able to interchange and distribute information throughout the swarm.

From the different types of swarms discussed so far (see Fig. 3), we specifically focused on the four types listed in Table 1.

Performance Measurements To measure the performance and efficiency of our swarms, we focused on two aspects: (1) the average time taken by the swarms to cross the finish line and, (2), the number of CRM's contraction-expansion cycles as a simple measurement of consumed energy. We varied the linear spring constant k and linear damping constant d of the CRMs (all connections had the same values) to evaluate the influence of the dynamic properties of the compliant connections on the performance and energy consumption.

Results

In the first set of experiments we investigated the average-time-to-pass performance of various swarms. For the angular springs, the spring and damping constants were kept to 0.19 and 5 respectively. The linear spring constant k was varied from [4, 37] Nm^{-1} with increments of 3 and the linear damping d was varied from [0,4] with increments of 1. We conducted 100 simulations for each combination of (k, d) pairs for all four types of swarms (see Table 1).

An episode started by placing the swarm at a random position and orientation at the starting line (i.e. the bottom of the simulation environment). The y-axis coordinate of the center of the swarm was initially constrained to zero, while the x-axis coordinate was changed randomly. A swarm was successful as soon as it passed the finish line (top of the simulation environment). The swarm was considered to have failed in the simulation, if it took longer than 60s.

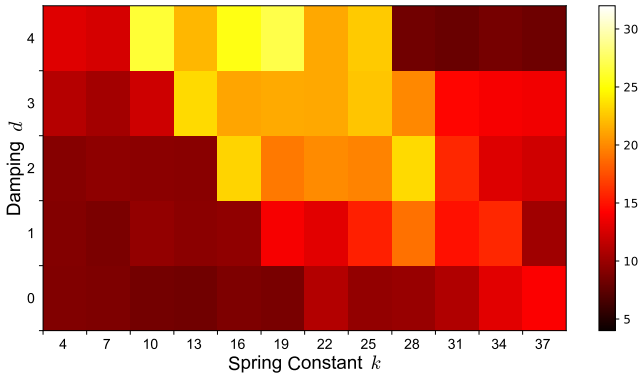

Figure 7: Type-P swarm: Effects of varying the linear spring and damping constants on the average time (in seconds) it takes for the swarm to cross the finish line.

Fig. 7 shows the average time taken by the swarm of type P (compliant, but passive) to cross the finish line for different (k, d) pairs. The lighter regions correspond to more time taken than the darker regions. Type-P swarms took a minimum of 7.7 s and a maximum of 27.8 s over all (k, d) pairs. It can also be seen that the best performance is region bound to $k : [5, 15], d : [0, 3]$ and $k : [28, 40], d : [4, 5]$ whereas the worst performance can be seen in the $k : [10, 30], d : [2, 5]$ region. In general, higher k increased the probability of the swarm getting stuck in the passage as the springs got stiffer. However, interestingly, there is also a region with higher k and higher d values (upper right corner in Fig. 7) where the average performance is good again. It can be argued that there exists a possibility of achieving better results either by increasing (see upper right corner, Fig. 7) or decreasing (k, d). However, the purpose of these experiments was to understand the *relative* performance of different swarms for the same range of (k, d) pairs. Furthermore, increasing k would make the springs stiffer and therefore make the swarm behave more like a passive swarm with rigid connections (see Fig. 3A), in which case they will not be able to cross the finish line.

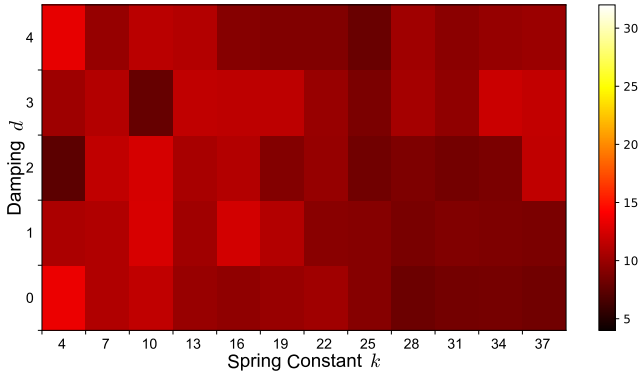

Figure 8: Type A_{rec} swarm: Effects of varying the spring and damping constants on the average time (in seconds) taken to cross the finish line.

Fig. 8 summarizes the same experiments, i.e. varying (k, d) values, for swarms of Type A_{rec} (compare to Fig. 3D). This type uses compliant connections, but, in addition, also has the capability to recoil from an obstacle through the previously described CRM mechanism. This additional property increases the performance significantly. Type A_{rec} swarms took a maximum of 13.8 s and a minimum of 7.45 s to reach the finish line for the investigated (k, d) values. Overall, the performance seems to be more homogeneous (see Fig. 8). There is no obvious trend for different k and d values. It seems the performance is nearly independent of the choice of stiffness and damping values. One possible explanation is that the previously bad performing region for type-P swarms (yellow colored region in Fig. 7) are removed due to the use of the retracting mechanism in swarm

type-A_{rec}.

We also investigated the ability of the swarms (type P and A_{rec}) to exhibit consistency in their performance. Fig. 9 shows the sample mean vs variance plot for type P and A_{rec} swarms for all investigated (k, d) pairs. The variance of the time taken by the type P swarm is large, which demonstrates their inability to consistently achieve similar results when compared to type A_{rec} swarms.

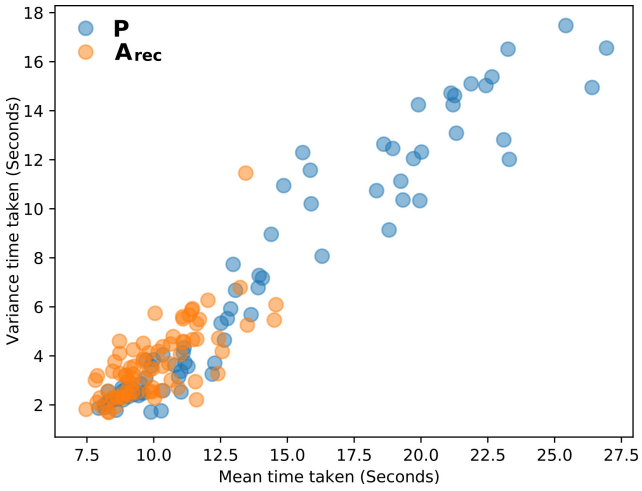

Figure 9: **The variance and average of the time taken to cross the finish line.** Type A_{rec} variance is clustered in a smaller area than type P demonstrating a higher constancy in their performance.

We carried out similar simulations for the type $A_{rec,osc}$ and A_{osc}, which use continuous oscillation. However, similar to A_{rec}, there were no trends observable with respect to the choice of k and d values. While the type $A_{rec,osc}$ took a maximum of 17.01s and a minimum of 8s, type A_{osc} took 18.67s and 10.47s respectively. Although the performance was quite similar between $A_{rec,osc}$ and A_{osc}, the major differences lie in the the energy consumption and emergent behaviour as discussed in the next sections.

Energy consumption

In addition to average passing time, we also evaluated the energy consumption of the different types of actively driven swarms to analyse their efficiency. Note that swarms of type P (Fig. 3B), which is completely passive, does not require any additional energy. The energy consumption was estimated by the number of expansion-contraction cycles of the CRMs. Furthermore, we did not calculate the actual energy used, but instead used a proportional measurement by counting the number of contractions performed. In these experiment we, (i) kept the damping constant to $d = 1$, which lies in the intersection of best performing regions of type P and A_{rec} and (ii) we varied the spring constant k for all CRMs from 5 to 40 Nm^{-1}. As a reminder, a CRM contracts either because of a collision detection as in type A_{rec}), or continuously oscillations as in type A_{osc} and $A_{rec,osc}$. Fig. 10 summarizes the results.

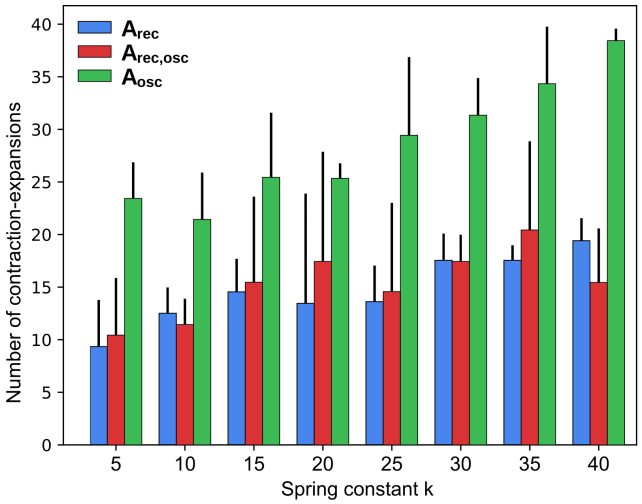

Figure 10: **Energy consumption**. Average number of expansion-contraction cycles for swarm types A_{rec}, $A_{rec,osc}$, and A_{osc} based on the chosen spring constant k.

We can see that type A_{rec} (blue) and $A_{rec,osc}$ (red) swarms have comparable energy consumption. In case of the $A_{rec,osc}$ swarms, oscillations are stopped when a collision is detected. Therefore, the energy consumption in them is comparable to A_{rec}. However, their most frequent emergent behaviors were significantly different (see next section). Unsurprisingly, the swarms of type A_{osc} exhibited the most contraction-expansion cycles (i.e. highest energy consumption), because the oscillation was constantly on.

Emergent behavior

As previously pointed out, some types of swarms performed similarly when looking at the average time and energy consumption. However, their cooperative behaviours, i.e. how they solved the task were different; some of them beneficial, others detrimental. For example, in case of type P swarms, for a given stiffness k (i.e., a row in the Fig. 7), when we increase the damping d, in general, the performance worsens. This is related to an emergent behavior which could be consistently observed in the simulation of type P swarms. A single robot of the swarm would cross the passage first, while the other two remained stuck in the passage (compare Fig. 11, frame 3). Then, because of the flow-field, the first robot, which was already out of the passage, would start to oscillate sideways, i.e., left-right-left (Fig. 11, frame 3-9). This would cause the other two robots eventually to shift inside and cross the passage as well (Fig. 11, frame 10-12). Consequently, higher damping values d reduced oscillations and were indirectly working against this strategy, therefore, lowering the performance. In addition, compliance plays a

key role here and morphological communication facilitates this process.

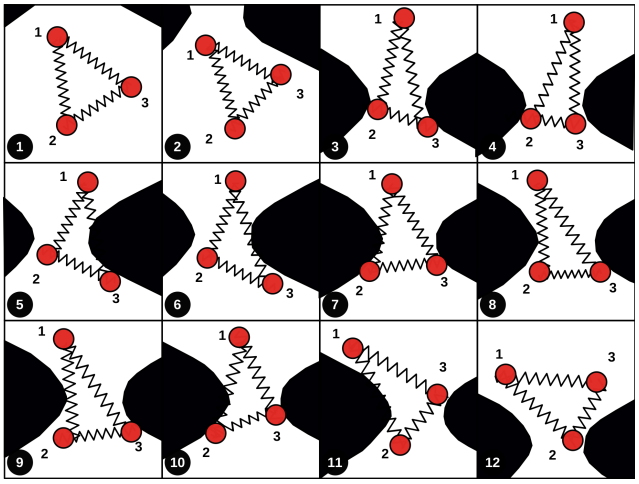

Figure 11: **Emergent behaviour of type P swarm.** The frame numbers are shown in circles with black infill. The type P swarm is completely passive.

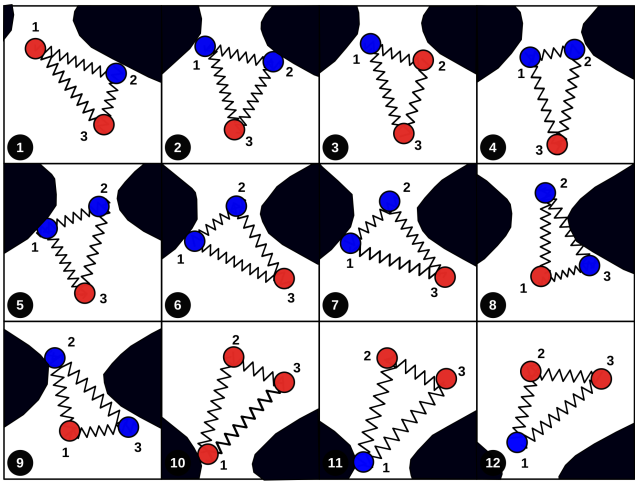

Figure 12: **Emergent behaviour of type A_{rec} swarm.** The frame numbers are shown in circles with a white background. Blue circle show when the retraction mechanisms was activated. Red when it was inactive.

The prevalent behaviour of type A_{rec} swarms is shown in Fig. 12. Under the influence of the flow field, the swarm moved towards the gap until one robot collided with either side of the terrain which due to contraction, pulled in at least one robot (see Fig. 12 frame 1-4; robot 1 collides and pulls in robot 2). The other robot which had not yet collided with the terrain, started rotating until a collision occurred with the terrain (see Fig. 12 frame 5-7; robot 3). This allowed the robots stuck in the passage to slightly shift, which allowed it to get through the passage (see Fig. 12 frame 8-9, robot 2). Finally, a recoil from the robot which recently passed through, pulled the other robot (see Fig. 12 frame 9-10; robot 2 pulls in robot 3).

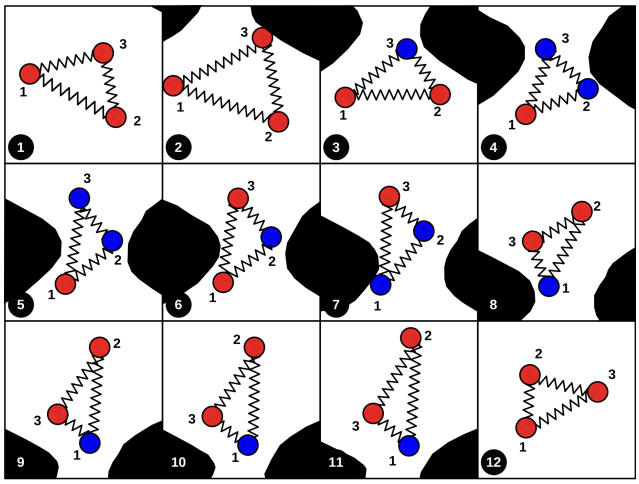

Figure 13: **Emergent behaviour of type $A_{rec,osc}$ swarm.**

For the $A_{rec,osc}$, both swarm collision detection and oscillation were enabled. This means, in the absence of a collision, all connections expanded and contracted uniformly and continuously. However, any collision caused a particular robot to contract and stop its oscillation for a small amount of time (see Fig. 13). Any other robots kept oscillating, pulling in the other robot due to the mixed influence of their own mass and the flow-field. This behaviour was also prevalent in the type A_{osc} where recoiling was disabled. Under the constant oscillations, as it approached the narrow passage, the swarm formed a cluster during the contraction half of the oscillation. This physically inhibited the expansion of at least one of the robots. The robots which were free to move in the environment, pulled the others through the passage.

Conclusion and Future Work

In this paper, we proposed morphological communication for swarms where agents share compliant physical connections. The motivation was to simplify the technological needs for communication which can potentially improve scalability. We investigated different types of swarms with different levels of control. We simulated completely passive swarms (type P), swarms that used sensing and a recoiling mechanism (type A_{rec}), swarms that blindly oscillated (type A_{osc}), and swarms that combined recoiling and oscillation (type $A_{rec,osc}$). They all used their compliant connections to transmit and distribute information about contact with the environment to the other agents. While the performance of completely passive swarms depended on stiffness and damping values, all the other swarms performed well for any of the tested stiffness/damping pairs.

We also estimated the energy consumption by counting

the number of contractions. Type A_{rec} and $A_{rec,osc}$ were quite similar in that respect, but type A_{osc}, which blindly oscillated even when it was not needed, had the highest estimated energy consumption. Furthermore, even though different types performed often similarly, we saw clear differences in their behaviours, i.e., how they solved the task. It seems different control policies led to different approaches. It's import to emphasize that these behaviors were not programmed into the systems. Rather, they emerged out of the interaction of the agents among each other and the environment – A principle that is often referred to as embodied intelligence (Pfeifer and Bongard (2006)) or morphological computation (Hauser et al. (2011)). Furthermore, morphological communication, i.e., processing information via local vibrations, does not consume energy as it is inherently handled by the morphology of the swarm. In a traditional swarms where information is conveyed through wireless communication protocols, energy is consumed both for transmission and processing. It can also be argued that, for swarms with agents below the millimeter scale, traditional motors (or mechanisms like CRMs) are hard to build and maintain. However, the principle of morphological communication doesn't necessary need mechanical springs and electrically facilitated recoiling mechanisms. At very small scales alternative implementations of CRMs are feasible, including the use of protocells or even biological cells (muscles, tendons, etc.), see, e.g. Hauser (2019).

Future work will include the investigation of more complex swarms with more agents. Furthermore, the extension to other more complex tasks is of interest as well.
Although mechanical connections constrain the agents, we believe the presented work demonstrates the potential for such an approach. We particularly believe that compliant morphological properties can improve the dynamic interactions between the agents about the environment. Therefore, providing a novel way to facilitate the emergence of interesting behaviors in swarms especially in applications such as nano-medicine, where scale becomes a primary constraint.

References

Alattas, R. (2018). Analyzing modular robotic systems. In *Online Engineering & Internet of Things*, pages 1014–1028. Springer.

Asheesh, S. and Helmut, H. (2020). Asheeshkrsharma/morphological-communication. *2020 Zenodo*.

Bentley, K., Harrington, K., and Regan, E. (2014). Can active perception generate bistability? heterogeneous collective dynamics and vascular patterning. *Artificial Life Conference Proceedings*, (26):328–335.

Brambilla, M., Ferrante, E., Birattari, M., and Dorigo, M. (2013). Swarm robotics: a review from the swarm engineering perspective. *Swarm Intelligence*, 7(1):1–41.

Brown, H. B., Vande Weghe, J. M., Bererton, C. A., and Khosla, P. K. (2002). Millibot trains for enhanced mobility. *IEEE/ASME Transactions on Mechatronics*, 7(4):452–461.

Caluwaerts, K. and Schrauwen, B. (2011). The body as a reservoir: locomotion and sensing with linear feedback. *Proceedings of the 2nd International Conference on Morphological Computation (ICMC 2011)*.

Catto, E. (2011). Box2d: A 2d physics engine for games. *URL: http://www.box2d.org*.

Chennareddy, S., Agrawal, A., and Karuppiah, A. (2017). Modular self-reconfigurable robotic systems: a survey on hardware architectures. *Journal of Robotics*, 2017.

Cianci, C. M., Raemy, X., Pugh, J., and Martinoli, A. (2006). Communication in a swarm of miniature robots: The e-puck as an educational tool for swarm robotics. In *International Workshop on Swarm Robotics*, pages 103–115. Springer.

Couceiro, M. S. (2017). An overview of swarm robotics for search and rescue applications. In *Artificial Intelligence: Concepts, Methodologies, Tools, and Applications*, pages 1522–1561. IGI Global.

Deblais, A., Barois, T., Guerin, T., Delville, P.-H., Vaudaine, R., Lintuvuori, J. S., Boudet, J.-F., Baret, J.-C., and Kellay, H. (2018). Boundaries control collective dynamics of inertial self-propelled robots. *Physical Review Letters*, 120(18):188002.

Duarte, M., Gomes, J., Costa, V., Rodrigues, T., Silva, F., Lobo, V., Marques, M. M., Oliveira, S. M., and Christensen, A. L. (2016). Application of swarm robotics systems to marine environmental monitoring. In *OCEANS 2016-Shanghai*, pages 1–8. IEEE.

Floreano, D., Mitri, S., Magnenat, S., and Keller, L. (2007). Evolutionary conditions for the emergence of communication in robots. *Current Biology*, 17(6):514 – 519.

Garattoni, L. and Birattari, M. (2018). Autonomous task sequencing in a robot swarm. *Science Robotics*, 3(20).

Hauert, S. and Bhatia, S. N. (2014). Mechanisms of cooperation in cancer nanomedicine: towards systems nanotechnology. *Trends in Biotechnology*, 32(9):448 – 455. Special Issue: Next Generation Therapeutics.

Hauert, S., Leven, S., Zufferey, J.-C., and Floreano, D. (2010). Communication-based swarming for flying robots. *Proceedings of the Workshop on Network Science and Systems Issues in Multi-Robot Autonomy, IEEE International Conference on Robotics and Automation*.

Hauert, S., Mitri, S., Keller, L., and Floreano, D. (2014). Evolving cooperation: From biology to engineering. Technical report, MIT press.

Hauser, H. (2019). Resilient machines through adaptive morphology. *Nature Machine Intelligence*.

Hauser, H., Ijspeert, A. J. A., Füchslin, R. M. R., Pfeifer, R., and Maass, W. (2011). Towards a theoretical foundation for morphological computation with compliant bodies. *Biological Cybernetics*, 105(5-6):355–370.

Hinchey, M. G., Sterritt, R., and Rouff, C. (2007). Swarms and swarm intelligence. *Computer*, 40(4):111–113.

Ishiguro, A., Umedachi, T., Kitamura, T., Nakagaki, T., and Kobayashi, R. (2008). A fully decentralized morphology control of an amoeboid robot by exploiting the law of conservation of protoplasmic mass.

Kaynaklarından, E., Alanlarına, U., Bölümü, B. M., and Ürk Iye, T. (2005). Swarm robotics: From sources of inspiration to domains of application.

Li, B., Ma, S., Liu, J., Wang, M., Liu, T., and Wang, Y. (2009a). Amoeba-i: A shape-shifting modular robot for urban search and rescue. *Advanced Robotics*, 23:1057–1083.

Li, S., Batra, R., Brown, D., Chang, H.-D., Ranganathan, N., Hoberman, C., Rus, D., and Lipson, H. (2019). Particle robotics based on statistical mechanics of loosely coupled components. *Nature*, 567:361–365.

Li, Y., Du, S., and Kim, Y. (2009b). Robot swarm manet cooperation based on mobile agent. In *2009 IEEE International Conference on Robotics and Biomimetics (ROBIO)*, pages 1416–1420. IEEE.

Owaki, D., Kano, T., Nagasawa, K., Tero, A., and Ishiguro, A. (2013). Simple robot suggests physical interlimb communication is essential for quadruped walking. *Journal of The Royal Society Interface*, 10(78).

Perlin, K. (2002). Improving noise. In *ACM Transactions on Graphics (TOG)*, volume 21, pages 681–682. ACM.

Pfeifer, R. and Bongard, J. C. (2006). *How the body shapes the way we think*. The MIT Press.

Rieffel, J. A., Valero-Cuevas, F. J., and Lipson, H. (2010). Morphological communication: exploiting coupled dynamics in a complex mechanical structure to achieve locomotion. *Journal of The Royal Society Interface*, 7(45):613–621.

Roberts, J. F., Stirling, T. S., Zufferey, J.-C., and Floreano, D. (2009). 2.5d infrared range and bearing system for collective robotics. *2009 IEEE/RSJ International Conference on Intelligent Robots and Systems*, pages 3659–3664.

Rubenstein, M., Cornejo, A., and Nagpal, R. (2014). Programmable self-assembly in a thousand-robot swarm. *Science*, 345(6198):795–799.

Seo, J., Paik, J., and Yim, M. (2019). Modular reconfigurable robotics. *Annual Review of Control, Robotics, and Autonomous Systems*, 2(1):63–88.

Slavkov, I., Carrillo-Zapata, D., Carranza, N., Diego, X., Jansson, F., Kaandorp, J., Hauert, S., and Sharpe, J. (2018). Morphogenesis in robot swarms. *Science Robotics*, 3(25).

Trenkwalder, S. M., Esnaola, I., Lopes, Y. K., Kolling, A., and Groß, R. (2020). Swarmcom: an infra-red-based mobile ad-hoc network for severely constrained robots. *Autonomous Robots*, 44(1):93–114.

Tutuko, B. and Nurmaini, S. (2014). Swarm robots communication-base mobile ad-hoc network (manet). *Proceeding of the Electrical Engineering Computer Science and Informatics*, 1(1):134–137.

Umedachi, T., Idei, R., and Ishiguro, A. (2012a). A true-slime-mold-inspired fluid-filled robot exhibiting versatile behavior. In Prescott, T. J., Lepora, N. F., Mura, A., and Verschure, P. F. M. J., editors, *Biomimetic and Biohybrid Systems*, pages 262–273, Berlin, Heidelberg. Springer Berlin Heidelberg.

Umedachi, T., Idei, R., Ito, K., and Ishiguro, A. (2013). True-slime-mould-inspired hydrostatically coupled oscillator system exhibiting versatile behaviours. *Bioinspiration & Biomimetics*, 8(3):035001.

Umedachi, T., Idei, R., Nakagaki, T., Kobayashi, R., and Ishiguro, A. (2012b). Fluid-filled soft-bodied amoeboid robot inspired by plasmodium of true slime mold. *Advanced Robotics*, 26(7):693–707.

Umedachi, T., Takeda, K., Nakagaki, T., Kobayashi, R., and Ishiguro, A. (2010a). Fully decentralized control of a soft-bodied robot inspired by true slime mold. *Biol. Cybern.*, 102(3):261–269.

Umedachi, T., Takeda, K., Nakagaki, T., Kobayashi, R., and Ishiguro, A. (2010b). A soft-bodied fluid-driven amoeboid robot inspired by plasmodium of true slime mold. In *2010 IEEE/RSJ International Conference on Intelligent Robots and Systems*, pages 2401–2406.